Available online at www.sciencedirect.com
SciVerse ScienceDirect
Journal of the Chinese Medical Association 76 (2013) 458–465
www.jcma-online.com

Original Article

Image quality improvement in three-dimensional time-of-flight magnetic resonance angiography using the subtraction method for brain and temporal bone diseases

Shu-Hui Peng [a,b], Chao-Yu Shen [a,b,c], Ming-Chi Wu [a,b,c], Yue-Der Lin [d], Chun-Huang Huang [e], Ruei-Jin Kang [f], Yeu-Sheng Tyan [a,b,c], Teng-Fu Tsao [a,b,c,g,*]

[a] Department of Medical Imaging, Chung Shan Medical University Hospital, Taichung, Taiwan, ROC
[b] School of Medical Imaging and Radiological Sciences, Chung Shan Medical University, Taichung, Taiwan, ROC
[c] Department of Radiology, School of Medicine, Chung Shan Medical University, Taichung, Taiwan, ROC
[d] Department of Automatic Control Engineering, Feng Chia University, Taichung, Taiwan, ROC
[e] Institute of Medicine, Chung Shan Medical University, Taichung, Taiwan, ROC
[f] National Chi Nan University, Puli, Nantou, Taiwan, ROC
[g] Department of Veterinary Medicine, National Chung Hsing University, Taichung, Taiwan, ROC

Received October 9, 2012; accepted December 28, 2012

Abstract

Background: Time-of-flight (TOF) magnetic resonance (MR) angiography is based on flow-related enhancement using the T1-weighted spoiled gradient echo, or the fast low-angle shot gradient echo sequence. However, materials with short T1 relaxation times may show hyperintensity signals and contaminate the TOF images. The objective of our study was to determine whether subtraction three-dimensional (3D) TOF MR angiography improves image quality in brain and temporal bone diseases with unwanted contaminations with short T1 relaxation times.
Methods: During the 12-month study period, patients who had masses with short T1 relaxation times noted on precontrast T1-weighted brain MR images and 24 healthy volunteers were scanned using conventional and subtraction 3D TOF MR angiography. The qualitative evaluation of each MR angiogram was based on signal-to-noise ratio (SNR), contrast-to-noise ratio (CNR) and scores in three categories, namely, (1) presence of misregistration artifacts, (2) ability to display arterial anatomy selectively (without contamination by materials with short T1 relaxation times), and (3) arterial flow-related enhancement.
Results: We included 12 patients with intracranial hematomas, brain tumors, or middle-ear cholesterol granulomas. Subtraction 3D TOF MR angiography yielded higher CNRs between the area of the basilar artery (BA) and normal-appearing parenchyma of the brain and lower SNRs in the area of the BA compared with the conventional technique (147.7 ± 77.6 vs. 130.6 ± 54.2, $p < 0.003$ and 162.5 ± 79.9 vs. 194.3 ± 62.3, $p < 0.001$, respectively) in all 36 cases. The 3D subtraction angiography did not deteriorate image quality with misregistration artifacts and showed a better selective display of arteries ($p < 0.0001$) and arterial flow-related enhancement ($p < 0.044$) than the conventional method.
Conclusion: Subtraction 3D TOF MR angiography is more appropriate than the conventional method in improving the image quality in brain and temporal bone diseases with unwanted contaminations with short T1 relaxation times.

Keywords: contamination; hematoma; magnetic resonance angiography; subtraction

* Corresponding author. Dr. Teng-Fu Tsao, Department of Medical Imaging, Chung Shan Medical University Hospital, 110, Section 1, Chien-Kuo North Road, Taichung 402, Taiwan, ROC.
E-mail address: cshy1069@csh.org.tw (T.-F. Tsao).

1726-4901/$ - see front matter
http://dx.doi.org/10.1016/j.jcma.2013.04.006

1. Introduction

Time-of-flight (TOF) magnetic resonance (MR) angiography is based on flow-related enhancement using the T1-weighted spoiled gradient echo or the fast low-angle shot gradient echo sequence. The technique is used widely and is considered an effective approach for imaging intracranial blood vessels.[1,2] However, materials with short T1 relaxation times may show hyperintensity signals and contaminate the TOF images.[3] Although not commonly used, a subtraction method has been introduced to remove hyperintense subacute hematoma from TOF MR angiographic images.[4] The purpose of this study was to investigate whether the subtraction method in three-dimensional (3D) TOF MR angiography can successfully remove unwanted contaminations in various brain and temporal bone conditions.

2. Methods

2.1. Patients and study protocol

Patients who had masses with short T1 relaxation times noted on precontrast T1-weighted brain MR images and 24 healthy volunteers were included in this 12-month prospective study. The study was approved by the Institutional Review Board of our hospital and written informed consent was obtained from all patients or their families.

All imaging examinations were performed with 1.5-T MR imagers (MAGNETOM Sonata, Siemens Medical Solutions, Erlangen, Germany, or Signa Horizon EchoSpeed, General Electric Medical Systems, Milwaukee, WI, USA) equipped with high-performance three-axis gradient systems. To obtain useful data we instructed patients on how to minimize head movements before MR scans. If needed, suitable sedation was achieved by following the general procedure in our hospital. The scan protocol included T1-weighted, T2-weighted, fluid attenuation inversion recovery, and diffusion-weighted imaging and both conventional and subtraction 3D TOF MR angiography sequences. Contrast-enhanced magnetic resonance imaging (MRI) and contrast-enhanced MR angiography were used, if indicated.

2.2. 3D TOF MR angiography protocol

Conventional 3D TOF MR angiography was performed with multiple thin axial slabs. The imaging parameters for the 3D TOF MR angiogram pulse sequence were repetition time/echo time, 37/7.2 ms; flip angle, 25°; slice per slab, 32; slice thickness, 1.1 mm; matrix size, 512 × 192; field of view, 220 × 165 mm; receiver bandwidth, 65 Hz/Px; number of excitations, 1; number of slabs, 3; acquisition time, 5.5 minutes. Flow compensation was used to minimize flow-related signal voids in the vessels. Magnetization transfer saturation was used to selectively saturate the static tissue and thus increase the vessel-to-background contrast.[5,6] Multiple overlapping thin-slab acquisition was performed sequentially to reduce the progressive saturation that occurs in the blood during its passage through the imaging slab.[1,7,8] Ramped radio-frequency excitation pulses with tilted optimized nonsaturating excitation were used to increase the flip angle across the 3D acquisition volume.[9,10] In addition, superior spatial saturation slabs were added to remove the contamination of venous flow.

A second set of MR angiograms was then acquired by repeating the data-acquisition procedure using the same pulse sequence and imaging parameters and identical slice locations, except that double (both superior and inferior) spatial saturation slabs were added. The double spatial saturation slabs were designed to create flow voids of all head blood vessels in the second set of MR angiograms.[4]

2.3. Image postprocessing

After data acquisition, the first set of conventional 3D TOF MR angiographic source images was subtracted from the second on a pixel-by-pixel basis using workstations provided by the manufacturers of the MR systems. This produced a third set of subtracted source images. The first and third sets were reconstructed with maximum-intensity-projection images in different views to obtain a conventional 3D TOF MR angiogram image and a subtraction 3D TOF MR angiogram image. All of the source and reconstructed images were sent to the hospital's picture archiving and communication systems for archiving and future review. There was no rudimentary image registration technique before image subtraction in our postprocessing program.

2.4. Image evaluation and data analysis

To evaluate objectively the quality of the 3D TOF MR angiographic maximum-intensity-projection images, signal-to-noise ratios (SNRs) and contrast-to-noise ratios (CNRs) were calculated on the basis of signal intensity (SI) measurements in manually drawn regions of interest (ROIs). ROIs were placed by an MR technician in areas of the basilar artery (BA) and normal-appearing parenchyma (NAP) of the brain, and the air outside the object. Noise (N) was defined as the standard deviation of the SI within air. The SNR and CNR values were calculated from the following equations: $\mathrm{SNR} = SI_{\mathrm{BA}}/N$ and $\mathrm{CNR} = (SI_{\mathrm{BA}} - SI_{\mathrm{NAP}})/N$, where SI_{BA} is SI in the area of the BA, SI_{NAP} is SI in the NAP of the brain, and N is noise.

To assess the quality of the 3D TOF MR angiographic maximum-intensity-projection images subjectively, images presented in a randomized fashion were reviewed separately by two neuroradiologists. Qualitative evaluation was based on modified criteria originally designed to evaluate contrast-enhanced MR angiograms.[11] The criteria were (1) presence of misregistration artifacts, (2) ability to display arterial anatomy selectively (without contamination by materials with short T1 relaxation times), and (3) arterial flow-related enhancement. For misregistration artifacts, images were assigned a score of 0 if there were no artifacts, 1 if artifacts were present but did not have a negative effect on the diagnosis, and 2 if they were present and did have a negative effect on the diagnosis. For the selective display of arteries without contamination, images were assigned a score of 0 if there was no contamination, 1 if there was contamination but it did not have a negative effect on the diagnosis, and 2 if there was contamination and it did have a negative effect on the diagnosis. For the arterial flow-related enhancement, images were assigned a score of 0 if flow-related enhancement was good, 1 if it was moderate, and 2 if it was poor. The two observers had the opportunity to review other MR images of cases in the scoring program when needed.

2.5. Statistical analysis

A statistician using standard statistical software (SPSS version 15.0 for Microsoft Windows, SPSS Inc., Chicago, IL, USA) performed the statistical analysis for this study. In the objective evaluation of quality, data are presented as means ± standard deviations. A paired *t* test was used to analyze observed differences. An analysis of interobserver agreement of qualitative variables was assessed by the kappa agreement test.[12] Mean scores data from the two observers were used for further analysis. The statistical significance of differences between conventional and subtraction 3D TOF MR angiography was established using the Wilcoxon signed-rank test in the qualitative evaluation.

3. Results

All imaging examinations, using both conventional 3D TOF MR angiography and subtraction 3D TOF MR angiography, were successfully completed. The study included 12 patients (six men and six women) with a mean age of 39.2 years (range: 1−82 years) and documented intracranial or temporal bone diseases (Table 1), and 24 healthy volunteers (11 men and 13 women) with a mean age of 55.2 years (range: 10−81 years) in our hospital. Seven patients had intracranial hematomas (Cases 2−6, 9, and 11) (Fig. 1), three had parasellar brain tumors (Cases 8, 10, and 12) (Fig. 2), and two had cholesterol granulomas of the middle ear (Cases 1 and 7) (Fig. 3). Using the subtraction technique, hyperintense hematomas and parasellar tumors or cholesterol granulomas with short T1 relaxation times and nonvascular natures were adequately removed from 3D TOF MR angiographic images. The circle of Willis can then be evaluated better.

Table 1
Summary of patient data and imaging findings in 12 patients.

Case Number	Gender/age (y)	Imaging findings
1	Female/15	Cholesterol granuloma, temporal bone
2	Male/82	Intracerebral hemorrhage
3	Male/53	Intracerebral hemorrhage
4	Male/40	Intracerebral hemorrhage
5	Female/33	Intracerebral hemorrhage
6	Male/52	Intracerebral hemorrhage
7	Female/13	Cholesterol granuloma, temporal bone
8	Female/49	Parasellar tumor
9	Male/65	Intracerebral hemorrhage
10	Female/11	Parasellar tumor
11	Male/1	Intracerebral hemorrhage and subdural hematoma
12	Female/44	Parasellar tumor

3.1. Objective comparison of image quality between conventional and subtraction TOF MR angiography

The results of SNR and CNR calculations for conventional and subtraction 3D TOF MR angiography are shown in Table 2. Subtraction 3D TOF MR angiography yielded significantly diminished SI in the area of the BA and NAP of the brain, and decreased noise compared with conventional 3D TOF MR angiography ($p < 0.001$). Subtraction 3D TOF MR angiography yielded significantly poorer SNR in the area of the BA compared with conventional 3D TOF MR angiography (162.5 ± 79.9 vs. 194.3 ± 62.3, $p < 0.001$). CNR measurements demonstrated a significantly higher contrast between the area of the BA and NAP of the brain with subtraction 3D TOF MR angiography compared with conventional 3D TOF MR angiography (147.7 ± 77.6 vs. 130.6 ± 54.2, $p < 0.003$).

3.2. Evaluating interobserver agreement in image quality

Interobserver agreement on the qualitative variables for the images (kappa index) is shown in Table 3. Interobserver agreement was perfect with respect to misregistration artifacts in both conventional and subtraction 3D TOF MR angiography ($\kappa = 1.000$); the data from the two neuroradiologists were completely identical. Interobserver agreement was substantial with respect to selective display of arteries ($\kappa = 0.649$ and 0.776 for conventional and subtraction 3D TOF MR angiography, respectively; substantial agreement). Interobserver agreement was moderate with respect to arterial flow-related enhancement ($\kappa = 0.490$ and 0.488 for conventional and subtraction 3D TOF MR angiography, respectively; moderate agreement).

3.3. Subjective comparison of image quality between conventional and subtraction TOF MR angiography

Qualitative results for conventional and subtraction 3D TOF MR angiography are shown in Table 4. Because conventional 3D TOF MR angiography does not use subtraction, it is not surprising that no misregistration artifacts (a score of 0) were observed for the images. By contrast, the two observers did not find any misregistration artifacts (a score of 0) in the subtraction 3D TOF MR angiography images. Subtraction 3D TOF MR angiography did not deteriorate image quality with misregistration artifacts.

With the selective display of arteries, the two observers noted, respectively, that 21 of 36 (58.3%) and 27 of 36 (75%) conventional 3D TOF MR angiography examinations showed contamination by short T1 materials with no negative effect on the diagnosis (a score of 1). By contrast, both observers

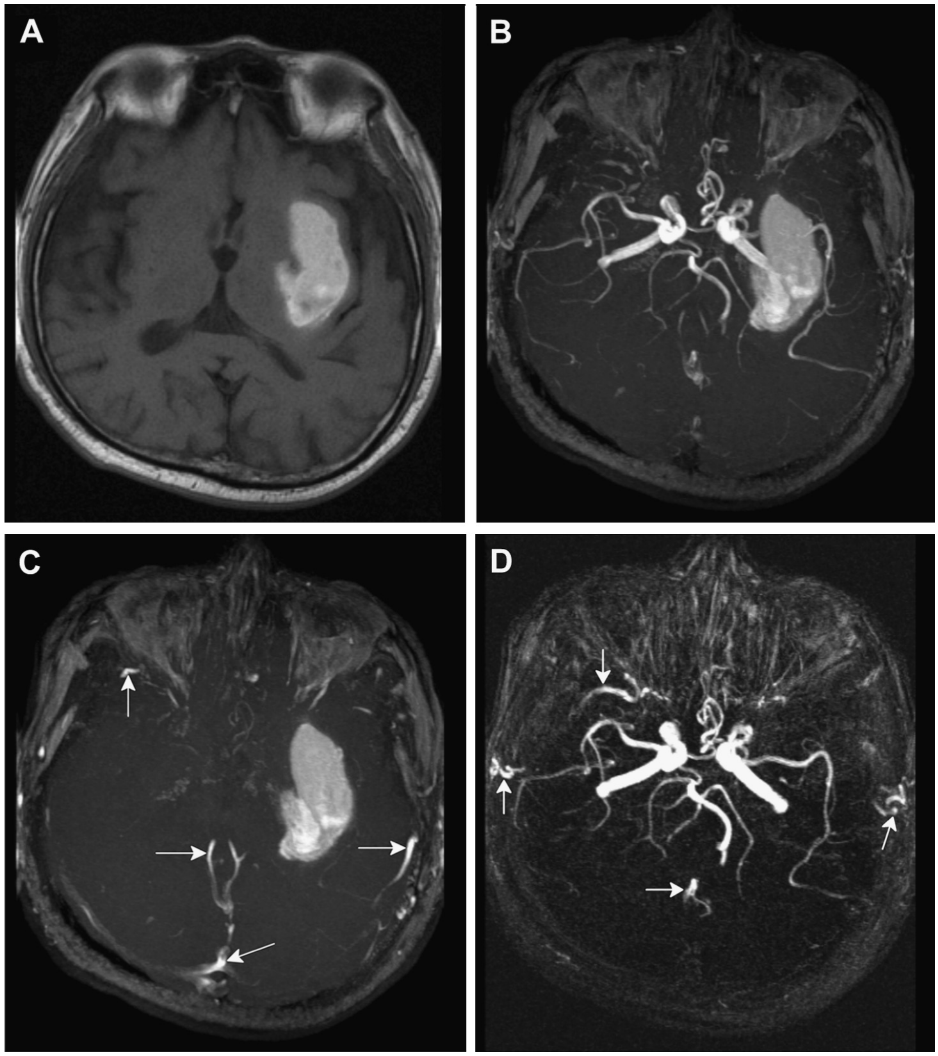

Fig. 1. Intracerebral hemorrhage in a 65-year-old male who presented with acute-onset right-sided weakness. (A) Axial T1-weighted image through the basal ganglia showing a short T1 hematoma in the left cerebrum. (B) Axial conventional three-dimensional (3D) time-of-flight magnetic resonance (TOF MR) angiogram of the circle of Willis showing a large short T1 hematoma obscuring the M1 segment of the left middle cerebral artery. For the selectively displayed arterial anatomy, both observers assigned the image quality scores of 2. (C) Axial second set 3D TOF MR angiogram acquired with both superior and inferior spatial saturation slabs showing most blood vessels as dark. The short T1 hematoma still appears bright. Multiple high signals (arrows) from the inflowing venous system were inadvertently not removed in the case. (D) Axial subtraction 3D TOF MR angiogram clearly showing the M1 segment of the left middle cerebral artery after removal of the hematoma. There is no aneurysm in the circle of Willis. The inadvertent high-signal venous contaminations in the second set of MR angiograms do not affect the subtraction MR angiogram with our technique. Even so, there are still some venous structures (arrows) from incomplete suppression on the image. For the selectively displayed arterial anatomy, both observers assigned the image quality scores of 0.

reported that 22 of 36 (61.1%) subtraction 3D TOF MR angiography examinations showed no contamination by short T1 materials (a score of 0). Subtraction 3D TOF MR angiography yielded significantly better scores for the selective display of arteries ($p < 0.0001$).

With respect to arterial flow-related enhancement, the two observers noted, respectively, that 21 of 36 (58.3%) and 18 of 36 (50%) conventional 3D TOF MR angiography examinations revealed only moderate flow-related enhancement (a score of 1). By contrast, although 21 of 36 (58.3%) subtraction 3D TOF MR angiography examinations revealed only moderate flow-related enhancement, according to the observer 1 (a score of 1), the number of cases with good flow-related enhancement (a score of 0) increased from 8 to 11 after using the subtraction technique, whereas the number of cases with poor flow-related enhancement (a score of 2) decreased from 7 to 4. The observer 2 reported that 20 of 36 (55.6%) subtraction 3D TOF MR angiography examinations showed good flow-related enhancement (a score of 0). Subtraction 3D TOF MR angiography yielded significantly better scores for arterial flow-related enhancement ($p < 0.044$) than did conventional 3D TOF MR angiography.

4. Discussion

Chan et al introduced subtraction 3D TOF MR angiography in 2003 for patients with subacute cerebral hemorrhage.[4] In their report, hyperintense subacute hematomas with

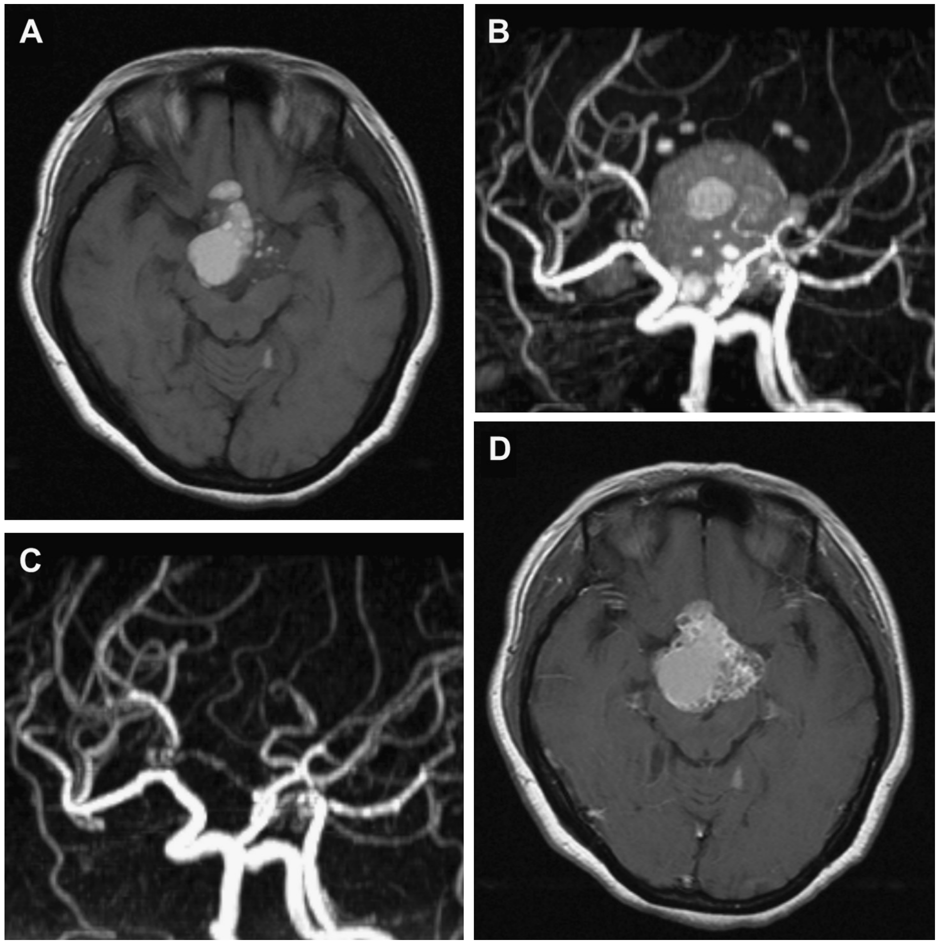

Fig. 2. Parasellar tumor in a 44-year-old female who presented with blurred vision for 2 years. (A) Axial T1-weighted image through the suprasellar cistern showing a lobulated mass containing multiple short T1 nodules in the midline. (B) Oblique sagittal conventional three-dimensional (3D) time-of-flight magnetic resonance (TOF MR) angiogram of the circle of Willis showing multiple aneurysm-like structures in the brain. For the selectively displayed arterial anatomy, both observers assigned the image quality scores of 2. (C) Oblique sagittal subtraction 3D TOF MR angiogram showing a normal circle of Willis. For the selectively displayed arterial anatomy, both observers assigned the image quality scores of 0. (D) Gadolinium-enhanced axial T1-weighted image showing multiple ring-enhancing cystic structures around the mass. The aneurysm-like structures in the conventional 3D TOF MR angiogram (B) are thought to be short T1 components within a tumor rather than true aneurysms with flow-related enhancements.

methemoglobin were adequately removed from 3D TOF MR angiographic images. Our study demonstrated similar results. In addition to hemorrhage, tumors with short T1 relaxation times may be related to the presence of intratumoral bleeding with intra- or extracellular methemoglobin or a cystic component with a high concentration of protein, fat, and/or calcification.[13] Data from our cases support the use of the subtraction technique for such clinical applications.

Because of the nonspecific soft-tissue pattern on computed tomography (CT) images, MRI is widely used in preoperative evaluation and postoperative follow-up of cholesterol granulomas.[14–16] Masses with high SI in the middle-ear cavities on both T1- and T2-weighted images are characteristic of cholesterol granulomas. However, the high SI, which is thought to be due to the paramagnetic effect of methemoglobin, may contaminate 3D TOF angiography, as occurred in our cases. Without careful evaluation, using only 3D TOF angiographic images may result in erroneously interpreting the diagnosis as a vascular lesion. At our institution, subtraction 3D TOF MR angiography can be used to explain the nonvascular nature of the lesion.

The major disadvantage of subtraction 3D TOF MR angiography is the long scan time needed for acquiring two sets of 3D TOF MR angiograms. The long scan time may further increase the risk of misregistration artifacts. To obtain useful data, we followed the suggestions of Chan et al.[4] We instructed patients on how to minimize head movements before the MR scans, and the second set of 3D TOF MR angiograms with double spatial saturation slabs was always immediately followed by conventional 3D TOF MR angiograms to minimize the time gap between the two sequences. Suitable sedation was achieved before MR scans, if indicated, by following the general procedure in our hospital. This may explain why the two observers reported that subtraction 3D TOF MR angiography showed no misregistration artifacts in any of the cases in our study.

Our data also showed that subtraction 3D TOF MR angiography yielded significantly better arterial flow-related

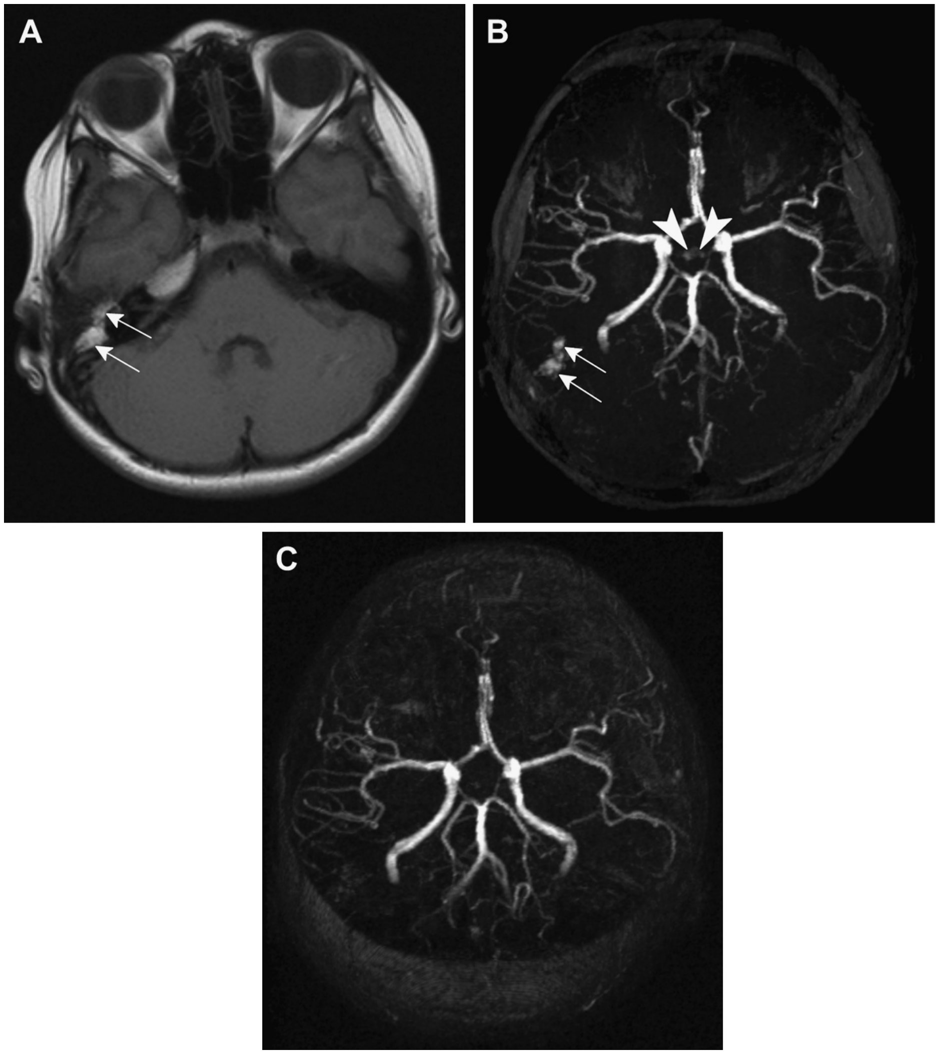

Fig. 3. Cholesterol granuloma in a 13-year-old female who presented with right hearing loss for a long time. (A) Axial T1-weighted image through the cerebellopontine angles showing a dumbbell mass (arrows) with short T1 contents in the right middle-ear cavity and adjacent mastoid antrum. (B) Axial conventional three-dimensional (3D) time-of-flight magnetic resonance (TOF MR) angiogram showing a suspected vascular lesion (arrows) in the right temporal bone. The high signal intensity (SI) of the posterior pituitary lobe (arrowheads) can be visualized. (C) Axial subtraction 3D TOF MR angiogram showing no obvious vascular lesion in the right temporal bone. The suspected vascular lesion on the conventional MR angiogram (B) has disappeared, indicating that it was a tumor mass. The high SI of the posterior pituitary lobe was also removed by the subtraction method.

enhancement than did conventional 3D TOF MR angiography. We believe this result may be attributed to the high CNR with the extensive suppression of the background MR signals in subtraction 3D TOF MR angiography. The low SNR in the subtraction technique seemed subjectively acceptable in our study.

The limitations of this study should be noted. As previously mentioned, all of the patients were very cooperative. Alert but uncooperative patients were usually referred for CT scans by physicians in our hospital. This was a selection bias of our study. In addition, all patients with intracranial diseases were diagnosed based on imaging studies. Surgical interventions

Table 2
Results of SNR and CNR calculation for conventional and subtraction TOF MR angiography.

Parameter	Conventional TOF MR angiography	Subtraction TOF MR angiography	*p*
SI in area of BA	446.4 ± 113.0	344.3 ± 102.8	<0.0001
SI in NAP	146.9 ± 30.7	32.3 ± 13.9	<0.0001
Noise	2.4 ± 0.4	2.2 ± 0.4	<0.0001
SNR in area of BA	194.3 ± 62.3	162.5 ± 79.9	<0.0001
CNR between area of BA and NAP	130.6 ± 54.2	147.7 ± 77.6	<0.003

Unless otherwise specified, data are means ± standard deviations. The *p* values are calculated with paired *t* test. BA = basilar artery; CNR = contrast-to-noise ratio; NAP = normal-appearing parenchyma; SI = signal intensity; SNR = signal-to-noise ratio; TOF MR = time-of-flight magnetic resonance.

Table 3
Interobserver agreement for image qualitative variables (kappa index).

	Image quality	Interobserver agreement	*p*
Conventional TOF MR angiography	Misregistration artifacts	1.000	
	The selective display of arteries	0.649	<0.0001
	Arterial flow-related enhancement	0.490	<0.0001
Subtraction TOF MR angiography	Misregistration artifacts	1.000	
	The selective display of arteries	0.776	<0.0001
	Arterial flow-related enhancement	0.488	<0.0001

TOF MR = time-of-flight magnetic resonance.

Table 4
Qualitative results for conventional and subtraction TOF MR angiography.

	Conventional TOF MR angiography		Subtracted TOF MR angiography	
	Observer 1	Observer 2	Observer 1	Observer 2
Misregistration artifacts				
0, no artifacts	36	36	36	36
1, artifacts presented without a negative effect on the diagnosis	0	0	0	0
2, artifacts presented with a negative effect on the diagnosis	0	0	0	0
The selective display of arteries				
0, no contamination by the material with short T1 relaxation time	1	1	22	22
1, contamination presented without a negative effect on the diagnosis	21	27	13	13
2, contamination presented with a negative effect on the diagnosis	14	8	1	1
Arterial flow-related enhancement				
0, good	8	15	11	20
1, moderate	21	18	21	14
2, poor	7	3	4	2

Data are number of participants. TOF MR = time-of-flight magnetic resonance.

for patients with parasellar tumors were not performed in our hospital and the types of tumors were not clear in our study. Only one of the patients with cholesterol granuloma received surgical treatment, allowing for confirmation by a pathological examination. In addition, the objective evaluation of the study was not performed on a per-vessel-segment basis. Only the SI in the area of the BA was measured because other intracranial arteries might be a little too small to be manually drawn adequately. Finally, the sample size in this study was small.

In conclusion, the results of our study suggest that subtraction 3D TOF MR angiography is more efficacious than conventional 3D TOF MR angiography for the evaluation of brain and temporal bone diseases with various unwanted contaminations with short T1 relaxation times. The subtraction technique yields a better selective display of arteries and arterial flow-related enhancement with higher CNR and lower SNR than does the conventional method. In addition, it does not deteriorate image quality with misregistration artifacts. We believe that subtraction 3D TOF MR angiography is an effective solution for clinical application in select patients.

Acknowledgments

This work was supported in part by a grant (Grant No. CSH-2009-A-015) from the Chung Shan Medical University Hospital, Taichung, Taiwan.

References

1. Handelsman H. Magnetic resonance angiography: vascular and flow imaging. *Health Technol Assess (Rockv)* 1994:1–20.
2. Heiserman JE, Drayer BP, Keller PJ, Fram EK. Intracranial vascular stenosis and occlusion: evaluation with three-dimensional time-of-flight MR angiography. *Radiology* 1992;**185**:667–73.
3. Lirng JF. Magnetic resonance venography of intracranial venous diseases. *J Chin Med Assoc* 2010;**73**:289–91.
4. Chan JH, Peh WC, Tsui EY, Wong KP, Yuen MK. Three-dimensional time-of-flight subtraction angiography of subacute cerebral hemorrhage. *AJR Am J Roentgenol* 2003;**181**:242–4.
5. Edelman RR, Ahn SS, Chien D, Li W, Goldmann A, Mantello M, et al. Improved time-of-flight MR angiography of the brain with magnetization transfer contrast. *Radiology* 1992;**184**:395–9.
6. Pike GB, Hu BS, Glover GH, Enzmann DR. Magnetization transfer time-of-flight magnetic resonance angiography. *Magn Reson Med* 1992;**25**:372–9.
7. Davis WL, Blatter DD, Harnsberger HR, Parker DL. Intracranial MR angiography: comparison of single-volume three-dimensional time-of-flight and multiple overlapping thin slab acquisition techniques. *AJR Am J Roentgenol* 1994;**163**:915–20.
8. Wu EX, Hui ES, Cheung JS. TOF-MRA using multi-oblique-stack acquisition (MOSA). *J Magn Reson Imaging* 2007;**26**:432–6.
9. Priatna A, Paschal CB. Variable-angle uniform signal excitation (VUSE) for three-dimensional time-of-flight MR angiography. *J Magn Reson Imaging* 1995;**5**:421–7.
10. Goodrich KC, Blatter DD, Parker DL, Du YP, Meyer KJ, Bernstein MA. A quantitative study of ramped radio frequency, magnetization transfer, and slab thickness in three-dimensional time-of-flight magnetic resonance angiography in a patient population. *Invest Radiol* 1996;**31**:323–32.
11. Van Hoe L, De Jaegere T, Bosmans H, Stockx L, Vanbeckevoort D, Oyen R, et al. Breath-hold contrast-enhanced three-dimensional MR

angiography of the abdomen: time-resolved imaging versus single-phase imaging. *Radiology* 2000;**214**:149−56.

12. Deshpande KK, Summers RM, Van Uitert RL, Franaszek M, Brown L, Dwyer AJ, et al. Quality assessment for CT colonography: validation of automated measurement of colonic distention and residual fluid. *AJR Am J Roentgenol* 2007;**189**:1457−63.
13. Bonneville F, Cattin F, Marsot-Dupuch K, Dormont D, Bonneville JF, Chiras J. T1 signal hyperintensity in the sellar region: spectrum of findings. *Radiographics* 2006;**26**:93−113.
14. Martin N, Sterkers O, Mompoint D, Julien N, Nahum H. Cholesterol granulomas of the middle ear cavities: MR imaging. *Radiology* 1989;**172**:521−5.
15. Campos A, Armengot M, Zapater E, Hostalet F, Basterra J. Cholesterol granuloma of the middle ear: report of 5 cases. *Acta Otorhinolaryngol Belg* 1996;**50**:125−9.
16. Pisaneschi MJ, Langer B. Congenital cholesteatoma and cholesterol granuloma of the temporal bone: role of magnetic resonance imaging. *Top Magn Reson Imaging* 2000;**11**:87−97.